Atmos. Chem. Phys. Discuss., 6, 7657–7695, 2006
www.atmos-chem-phys-discuss.net/6/7657/2006/

Atmospheric Chemistry and Physics Discussions

Stratospheric variability and trends in IPCC model simulations

E. C. Cordero[1] **and P. M. de F. Forster**[2]

[1]Department of Meteorology, San Jose State University, San Jose, CA 95192, USA
[2]School of Earth and Environment, University of Leeds, Leeds, LS2 9JT, UK

Received: 24 July 2006 – Accepted: 6 August 2006 – Published: 9 August 2006

Correspondence to: E. C. Cordero (cordero@met.sjsu.edu)

Abstract

Atmosphere and Ocean General Circulation Model (AOGCM) experiments for the Intergovernmental Panel on Climate Change Fourth Assessment Report are analyzed using both 20th and 21st century model output to better understand model variability and assess the importance of various forcing mechanisms on stratospheric trends. While models represent the climatology of the stratosphere reasonably well in comparison with NCEP reanalysis, there are biases and large variability among models. In general, AOGCMs are cooler than NCEP throughout the stratosphere, with the largest differences in the tropics. Around half the AOGCMs have a top level beneath ~2 hPa and show a significant cold bias in their upper levels (~10 hPa) compared to NCEP, suggesting that these models may have compromised simulations near 10 hPa due to a low model top or insufficient stratospheric levels. In the lower stratosphere (50 hPa), the temperature variability associated with large volcanic eruptions is either absent (in about half of the models) or the warming is overestimated in the models that do include volcanic aerosols. There is general agreement on the vertical structure of temperature trends over the last few decades, differences between models are explained by the inclusion of different forcing mechanisms, such as stratospheric ozone depletion and volcanic aerosols. However, even when human and natural forcing agents are included in the simulations, significant differences remain between observations and model trends, particularly in the upper tropical troposphere (200 hPa–100 hPa), where, since 1979, models show a warming trend and the observations a cooling trend.

1 Introduction

General Circulation Models (GCMs) are important tools for assessing how natural and anthropogenic forcings affect our climate and their predictions form the basis of our knowledge of future climate change. Climate models have evolved and improved into the currently used coupled Atmosphere Ocean GCMs (AOGCMs). To better represent

ACPD

6, 7657–7695, 2006

the many physical processes, horizontal and vertical resolution has also increased. Current models whose data will be used in Intergovernmental Panel on Climate Change (IPCC) fourth assessment report (AR4) focus on simulating the response of the surface and troposphere. The stratosphere of most of these models tends to be poorly resolved. In contrast, past stratospheric ozone assessment reports (e.g., WMO, 2003) tend to use data from models that focus resolution on the stratosphere. For a number of reasons it is becoming increasingly apparent that accurate simulations of the stratosphere are important to determine the evolution of the surface climate and other aspects of climate change.

1) Stratospheric temperature trends may provide some of the best evidence for attributing climate change to humans (Ramaswamy et al., 2006; Santer et al., 2005; Shine et al., 2003; Tett et al., 1996). Different climate forcing mechanisms such as carbon dioxide and solar constant changes are more readily distinguishable in their stratospheric response, compared to their surface response, which is often very similar between forcing agents (e.g., Forster et al., 2000). Further, human and natural effects can also be readily distinguished in tropopause height changes, which are a product of the tropospheric warming and stratospheric cooling associated with many human forcing agents (Santer et al., 2003a, b).

2) It has been shown that stratospheric variability and changes, particularly in the Northern and Southern Hemisphere polar vortices can affect the weather and climate of the troposphere (e.g., Shindell and Schmidt, 2004; Thompson et al., 2005). In particular Thompson et al. (2005) and Gillett and Thompson (2003) showed that part of the surface cooling in and around Antarctica could be associated with stratospheric ozone loss affecting the stratospheric polar vortex. In addition, several papers (e.g., Miller et al., 2006; Stenchikov et al., 2002) show that strong tropical volcanic eruptions (e.g., Mt. Pinatubo) and ozone depletion can both affect the winter arctic oscillation in the Northern Hemisphere. However it also appears that a well resolved stratosphere is required to accurately produce the correct tropospheric response (Gillett et al., 2002; Sigmond et al., 2004)

3) Several forcing or feedback mechanisms have a component associated with the stratosphere. Modeling the effects of stratospheric ozone depletion and explosive volcanic eruptions have benefited from a better representation of the stratosphere (2001). Solar irradiance changes may also have an effect on surface climate through inducing dynamical changes in the stratosphere (Haigh, 2001; Haigh et al., 2005; Rind, 2002, 2004). It is also important to resolve stratospheric water vapor changes as these can have a large effect on surface climate, as well as in the stratosphere (e.g., Forster and Shine, 2002). For example Stuber et al. (2001) found that the ECHAM4 GCM had a very strong feedback associated with stratospheric water vapor increases resulting from tropopause temperature increases.

Pawson et al. (2000) designed an intercomparison to compare and characterize the stratosphere using GCMs from a variety of modeling groups. In this paper we repeat aspects of this intercomparison for the current IPCC AOGCMs which were not specifically designed for stratospheric simulation. To aid climate-change attribution, we then expand this intercomparison to look at temperature trends in the stratosphere simulated since 1958, and compare these to observations.

The primary goal of this paper is to evaluate the ability of the participating IPCC models to simulate the structure, variability and trends of the lower stratosphere during the 20th century. Understanding the strengths and weaknesses not only provides feedback to the modeling community, but can also communicate to the larger public the uncertainties of predictions for the 21st century. In Sect. 2, a brief description of the IPCC models and various observation-based datasets are given. Model simulations and their comparisons with observations are given in Sect. 3, while Sect. 4 is devoted to understanding the temperature trends in the stratosphere over the last three decades. Section 5 describes 21st century temperature trends, and Sect. 6 is a discussion regarding the vertical profile of temperature trends. We finish with our conclusions in Sect. 7.

ACPD
6, 7657–7695, 2006

2 Model and observed data

The analysis uses AOGCM simulations from the IPCC Model archive at the Program for Climate Model Diagnosis and Intercomparison (PCMDI). Nineteen AOGCM simulations submitted to the archive from groups in ten different countries are compared using wind and temperature fields from the climate of the 20th century experiments. These models incorporate various natural and anthropogenic forcings including changes in ozone distribution, greenhouse gases and aerosols distribution, although not all models incorporate all of these forcing mechanisms. A list of the model forcings directly relevant to the stratosphere is given in Table 1 and will be discussed further in the next section.

The submitted model simulations record data at 17 vertical levels in the atmosphere (1000, 925, 850, 700, 600, 500, 400, 300, 250, 200, 150, 100, 70, 50, 30, 20, 10 hPa). The actual model top and number and placement of stratospheric levels vary from model to model, and are shown in Fig. 1. While the majority of models do have a model top above 10 hPa, the number of levels above the tropopause and the vertical resolution varies widely. Of the 19 models, only eight have more than three levels above 10 hPa. This scarcity of model levels in the stratosphere may be a significant impairment to accurately resolving the large scale structure and variability of the stratosphere (Hamilton et al., 1999).

Observational climatologies of temperature are used from both satellite and radiosonde observations. These include data from the Microwave Sounding Unit (MSU) carried on the NOAA polar orbiting satellites. Retrievals from the MSU provide atmospheric temperature at broadly defined levels of the troposphere and lower stratosphere. In this study, we use a climatology of MSU temperature data compiled by Remote Sensing Systems (RSS, Mears et al., 2003, of channel 2 (MSU2) and channel 4 (MSU4) retrievals of monthly and zonally averaged gridded temperature anomalies between 1979–1999.

We use two radiosonde datasets compiled from the groups at the Hadley Centre

ACPD
6, 7657–7695, 2006

(HadAT2; Thorne et al., 2005) and the NOAA (RATPAC-A; Free et al., 2005). These datasets, which use subsets of the global radiosonde network and span the years 1958–2004, are compiled into monthly average temperature anomalies. While these recently developed radiosonde climatologies incorporate various adjustments to account for data inhomogeneities (Free et al., 2004), a recent analysis by Randel and Wu (2006) suggests a systematic cold bias in the RATPAC-A tropical lower stratospheric data compared to the MSU satellite observations. This potential cold bias in the tropical lower stratosphere radiosonde observations will be considered in the subsequent model comparisons. A further description of the uncertainties regarding the MSU and radiosonde observations is given in the discussion of Sect. 6.

The model data will also be compared to the National Center for Environmental Prediction /National Center for Atmospheric Research (hereafter NCEP) Reanalysis. The NCEP data are derived using atmospheric general circulation models in a data assimilation system using in-situ and remotely sensed observations (Kistler et al., 2001). The NCEP reanalysis is available from 1948, but for stratospheric comparisons, only since the beginning of satellite observations in 1979 are the data likely to be reliable for global stratospheric studies (Randel et al., 2004). Although the ERA-40 reanalysis dataset has a higher range of altitudes, there are not significant differences between NCEP and ERA-40 for the global and zonally averaged fields examined in this study, and thus we will restrict the presentation of our results to the NCEP reanalysis.

3 20th century climate: model intercomparison

The AOGCMs participating in the IPCC model comparison represent the most advanced and comprehensive set of climate simulations so far produced. Simulations for the 20th century have been compared with each other and with available observations. In Table 1, we identify a subset of forcings used in the IPCC simulations of the 20th century climate that directly influence the stratosphere. The information on model forcing was largely obtained from the IPCC model website, where modeling groups supplied

ACPD
6, 7657–7695, 2006

information about their runs. For model simulations where the supplied information did not appear to match the model temperature simulations, a note was made. While all the models include the steady increase in greenhouse gas forcing, the models differ in their inclusion of variations in stratospheric ozone depletion, volcanic aerosols and variations in solar radiation. In the following section, an analysis of model experiments is made to assess model performance and the role of various forcing processes.

Figure 2 shows a vertical profile of the annual average global temperature from the IPCC models and the model temperature bias with respect to the NCEP reanalysis. The temperature distribution is averaged between 1979–1999 and ranges from the surface to 10 hPa. The temperature distribution illustrates the delineation in lapse rate between the troposphere and stratosphere, and the minimum in temperature at the tropopause. Near the surface and throughout the middle troposphere, the IPCC models agree reasonably well with each other and are generally within 2–3 K of the NCEP reanalysis, while at higher altitudes, the spread among the models increases. For example, at 700 hPa, the range of IPCC models differ by only ~3 K, while at 200 hPa and 10 hPa, the models differ by 6 K and 17 K, respectively. Although the standard deviation in the NCEP reanalysis shows that the natural variability in global mean temperature is larger in the troposphere compared to the stratosphere, models have larger differences compared to each other and larger biases compared to NCEP in the stratosphere compared to the troposphere. In addition, the models generally underestimate the global temperature in the stratosphere, a common GCM characteristic observed in various model intercomparisons (e.g., Austin et al., 2003; Pawson et al., 2000). AOGCM temperatures throughout most of the upper to the middle troposphere are also cooler than NCEP, a result we will explore further in Sect. 4.

A comparison of zonally averaged temperatures averaged between 1979–1999 at 500 hPa and 50 hPa from the models and NCEP is displayed in Fig. 3. In the middle troposphere, the models are within 5 K of each other and the NCEP reanalysis, with the uncertainty in NCEP less than 5 K at all latitudes. At 500 hPa the largest difference between models and observations is seen at the polar NH, where the models are

ACPD
6, 7657–7695, 2006

consistently colder than NCEP. An evaluation of seasonal temperature variations (not shown) shows that during both December, January, February (DJF) and June, July, August (JJA), most models are cooler than NCEP in the NH, while in the SH, there does not appear a similar bias. In the stratosphere, the range of temperatures between models is larger than in the troposphere, with a spread in magnitude of about 11 K in the tropics and poles and a slightly smaller range at midlatitudes. As shown by the uncertainty in the NCEP reanalyses, the natural variability in the stratosphere and especially near the polar stratosphere is larger than in the troposphere.

At the poles, the models generally are in reasonable agreement with the NCEP analyses, with no apparent cold pole biases that was a feature of older versions of GCMs (e.g., Pawson et al., 2000). In fact, the corresponding winter (DJF) polar temperatures in the NH are almost all within the NCEP uncertainty, while in the SH, of the 11 models that are outside the NCEP uncertainty, eight of the model are biased warm. In the tropics, a majority of the model simulations are cooler than the reanalysis, and the model to model variability is larger than in the extratropics, while the natural variability in the tropics is actually smaller than in the poles. Thus, the cooling bias seen in the global average temperature (Fig. 2), at least at 50 hPa, is not from a cold pole bias, but rather more by biases in the tropical latitudes. The tendency changes at higher altitudes, where a cold pole bias is seen in many models. During DJF, 14/19 of the models are colder than the observed variability between 70–90° N, while during JJA, 14/19 are colder than the observed variability between 70–90° S. These results imply that model representation of the planetary wave spectrum in the lower stratosphere of the winter hemisphere may be reasonable, while higher up this may not be the case. A natural question is then what role does the location of the model lid and number of stratospheric levels have on these results?

To evaluate the potential role of the vertical resolution and location of the model lid on the structure of stratospheric temperature, we group the models into two categories based on the altitude of the model lid and then examine the seasonal temperature variation between models and NCEP at three latitude ranges (70–90° N, 30° N–30° S

ACPD
6, 7657–7695, 2006

and 70–90° S) during the winter of each hemisphere (Fig. 4). The first group is labeled "high" and has a model lid at or above 45 km (~2 hPa; indicated as high in Table 1) while the second group is labeled "low" has a model lid below 45 km. Figure 4 illustrates the results of this comparison showing the difference (model – NCEP) for the two model groups in the high latitude winter hemisphere. During DJF and JJA, the difference between models with low and high tops is only significant near 10 hPa, the top reporting altitude for the IPCC dataset. In both cases, the models with a lower top (and fewer stratospheric levels) have a cold bias at 10 hPa of nearly 15 K, while the higher top models have a corresponding cold bias of between 4–7 K. There does not seem to be any statistically significant bias at lower altitudes. For example, at 50 hPa, the differences in biases for the two model groups are around 2 K during both seasons and within the variability of the NCEP reanalyses. These results suggest that the location of the model top, or related to this the number of stratospheric levels, affects model structure near 10 hPa in the winter hemisphere.

The evolution of stratospheric winds is related to temperature variations and ultimately controlled by large scale wave activity. In Fig. 5, the annual cycle in zonal wind at 60° N and 60° S at 50 hPa is displayed for each of the IPCC models and the NCEP reanalysis for the years 1979–1999. In the NH, the winds are westerly and strongest during winter (DJF) and easterly and weak in the summer (JJA). By plotting each year on the same scale, the interannual variability can also be estimated. While overall there is reasonable agreement with NCEP in terms of the timing of the maximum westerly winds, there exist significant variations in the peak magnitude of the westerly winds and the magnitude of the interannual variability. The interannual variability in NH DJF winds range from ~6 m s^{-1} in the CSIRO model to almost 20 m s^{-1} in the MRI model, compared to NCEP which is also around ~20 m s^{-1}.

The variability in the SH is markedly different compared with the NH. The year to year variability of peak westerly winds ranges from 4–10 m s^{-1}, almost half the variability seen in the NH. The smaller variability in the SH polar winds indicates a weaker planetary wave spectrum and is generally consistent with observation (Newman and

ACPD
6, 7657–7695, 2006

Nash, 2005). While the maximum winds reach over 50 m s^{-1} in a couple of the models, the NCEP reanalysis maximum winds appears larger than all the models except the CCSM3 model. However, because few reliable radiosonde observations in the middle to high latitude southern hemisphere exist, biases may exist at these locations (Randel et al., 2004). At higher altitudes, the magnitude of the winter winds increases in both hemispheres, as does the range of variability between models.

A comparison between zonal winds at 60° N and 60° S (Fig. 5) suggests that while hemispheric variations between the poles are reasonably captured, important departures from the observed climatology exist. This suggests that variations in dynamics and the characterization of large scale waves in IPCC models may inhibit the ability of models to accurately resolve stratospheric variability and change.

4 20th century trends

The primary radiative forcing mechanisms responsible for global temperature changes in the stratosphere over the last three decades have been increases in well-mixed GHG concentrations, declines in stratospheric ozone, explosive volcanic eruptions and solar changes (e.g., Ramaswamy et al., 2006). Increases in stratospheric water vapor may also influence global temperature trends (e.g., Shine et al., 2003). As the future promises further changes in all of these forcing processes, temperatures in the stratosphere will continue to change.

Figure 6 shows the global temperature anomaly at 50 hPa from the IPCC models between the years 1950 and 1999. The temperature anomaly is computed with respect to the average temperature computed between 1985–1995. The model time series are identified by colored lines and the model trends, calculated between the years 1958–1999, are given in K $decade^{-1}$ next to the model name. Trends are determined from a linear regression, while a Student t-test is performed to determine if the trend is statistically significant. In cases where the trend is statistically significant at the 95% levels, an asterisk (*) is placed next to the trend. The heavy black solid and dashed

lines indicate the RATPAC-A and HadAT2 radiosonde observations respectively.

Model temperatures at 50 hPa show that the majority of models indicate some cooling since 1958, with generally larger cooling rates since 1980. The cooling trend ranges from −0.06 to −0.61 K decade^{-1} in models with statistically significant trends, compared to the radiosonde observations that both show a statistically significant cooling of ∼0.47 K decade^{-1}. Among the models examined, 14 out of 19 (12 out of 19) show a statistically significant cooling trend between 1958–1999 (1979–1999). However, among these models, the majority underestimate the observed radiosonde trend, with only four models (CSIRO-mk3.0; gfdl-cm2.0/2.1; ukmo-hadcm3) near or above the radiosonde trend. The two simulations by miroc3.2h/m were also close to the observed trend, but were not statistically significant probably due to high variability caused by excessive sensitivity to volcanoes.

The most apparent feature in the 50 hPa temperature time series outside of the cooling trend are the three warming perturbations corresponding to the volcanic eruptions of Mt. Agung (1963), El Chichón (1982) and Mt. Pinatubo (1991). The warming results from increases in the absorption of incoming solar radiation and the absorption of outgoing infrared radiation by volcanic aerosols (Ramaswamy et al., 2001). As indicated in the forcing table (Table 1), nine of the models used for the IPCC include volcanic perturbations, although it was reported that two other models also included volcanic perturbations and yet did not show any corresponding temperature response. The model warming associated with the Mt. Agung eruption in 1963 ranges from 0.5 K to 2.0 K compared to the radiosonde observations which warmed globally by about 0.8 K over a year. In the later eruptions, a similar magnitude of model temperature response is found, with the Mt. Pinatubo eruption providing the largest temperature response as seen by radiosonde observations and satellite observations (Free and Angell, 2002; Karl et al., 2006). Radiosonde observations after Mt. Pinatubo show a warming of about 1 K, while the models that include volcanic aerosols generally overestimate this temperature response: for the models including volcanic aerosols, the temperature increase from 1990 to 1992 ranges from 1.0 to 2.5 K.

ACPD
6, 7657–7695, 2006

At higher altitudes (10 hPa; not shown), cooling trends are consistently larger and the magnitude of temperature variations associated with volcanic perturbations is reduced. Qualitatively, the trend toward stronger cooling with altitude generally agrees with the results of Shine et al. (2003) at 10 hPa and will be discussed further below.

Global model trends at altitudes from the surface to 10 hPa calculated between 1958–1999 are compared with the corresponding radiosonde observations in Fig. 7. The 2-sigma uncertainty in the HadAT2 and RATPAC-A radiosonde trends are also shown. The radiosonde trends, which are in good overall agreement with each other, show warming within the troposphere between 0.1 to 0.2 K decade^{-1} at the surface to between 0.1 to 0.3 K decade^{-1} up to 250 hPa. Between 200 and 150 hPa, the crossover point between tropospheric warming and stratospheric cooling in both radiosonde observations are collocated, while there are large differences among the models. Above 100 hPa, atmospheric cooling increases with altitude up to about −0.5 K decade^{-1} at 50 hPa. Model predictions generally range from 0.05 to 0.2 K decade^{-1} at the surface to 0.1 to 0.3 K decade^{-1} at 250 hPa. In the upper levels, the range of model trends becomes wider, ranging from −0.6 to 0 K decade^{-1} at 50 hPa, compared to a radiosonde calculated trend of −0.5 K decade^{-1}. While the majority of models are within the 2-sigma uncertainty of the radiosonde observations in the lower and middle troposphere (e.g., at 500 hPa, 16/19 models are within the uncertainty), in the upper troposphere and lower stratosphere, the majority of models show not enough cooling and are outside the uncertainty (e.g., at 50 hPa, 4/19 models are within uncertainty). While a cooling bias in the temperature trends derived from radiosonde observations may exist (e.g., Randel and Wu, 2006; Seidel et al., 2004), most models simulate the past stratospheric temperature trends quite poorly.

A potential explanation for why some of the models used for the IPCC compare poorly to radiosonde temperature trends is the absence of stratospheric ozone depletion (Ramaswamy et al., 2006; Shine et al., 2003). As illustrated in Table 1, of the 19 models that we compare for the 20th century, all models include well-mixed greenhouse gas forcing while only 11 include stratospheric ozone depletion. To explore this further,

ACPD
6, 7657–7695, 2006

temperature trends for models with and without ozone depletion are compared in Fig. 8 for the two time periods of 1958–1999 and 1979–1999. The simulations are separated based on the inclusion of stratospheric ozone depletion and model temperature trends are averaged in these two groups. The temperature trends from the RATPAC-A and HadAT2 radiosonde observations are also averaged, and the 2-sigma estimate of the trend uncertainty is indicated using horizontal lines. For the calculations of temperature trend between 1979–1999, satellite-derived trends computed from the RSS MSU analyses and their 2-sigma uncertainty are also shown, along with the approximate vertical range of these observations.

In the trend calculations for both time periods, the models that include ozone depletion are significantly closer to the observations than the models that omit ozone variations. In the trend between 1958–1999, the 50 hPa trend for the models with ozone depletion average almost $-0.4\,\mathrm{K\ decade^{-1}}$ while the models without ozone depletion are around $-0.1\,\mathrm{K\ decade^{-1}}$. In this case, the models with ozone depletion are within the range of uncertainty for the radiosonde observations. In the lower stratosphere/upper troposphere near (150–100 hPa), even models with ozone depletion fall outside the uncertainty of radiosonde observations, while below 150 hPa, the models with ozone depletion are within the radiosonde uncertainty and the models without ozone depletion remain outside the observations all the way down to 700 hPa.

The crossover point between the tropospheric warming and stratospheric cooling is also significantly different between the two model groups. The models with ozone depletion show a crossover point at around 150 hPa, while the models without ozone depletion show a crossover point at 70 hPa or about 4.8 km higher in altitude. From 200 hPa down to the surface, the models including ozone depletion are within the range of uncertainty for the radiosonde observations, while the models without ozone depletion are warmer than the observations down to 500 hPa.

The global trends computed for the years 1979–1999 show a similar overall pattern compared to the 1958–1999 data, although the rate of the tropospheric warming and stratospheric cooling is greater over the last two decades. The larger stratospheric

cooling since 1979 is not surprising considering most ozone depletion has occurred since 1979. In addition, the models also show better agreement to each other, and with both radiosonde and satellite observations from the surface to 300 hPa. At higher altitudes, however, the spread between the two model groups is larger than during 1958–1999. At 50 hPa, the temperature trend is −0.6 K decade^{-1} for the models with ozone depletion and −0.1 K decade^{-1} for the models without ozone trends, while the radiosonde and satellite observations are −0.8 K decade^{-1} and −0.45 K decade^{-1} respectively. These results are qualitatively consistent with Shine et al. (2003) who found significant divergence in the magnitude of model derived vertical temperature trends even when the same ozone trend datasets were employed in different models. As discussed previously, it has been suggested that radiosonde trends in stratospheric cooling may be too large as a result of instrument biases at tropical latitudes (Randel et al., 2006). Indeed there is better agreement between the models and the satellite observations, although at 70 hPa, the models including ozone depletion are within the uncertainty of both observational datasets.

Temperature trends in the tropics (30° N–30° S) calculated between 1979–1999 are shown in Fig. 9. From 50 hPa up to 10 hPa, the results look quite similar to the global model trends. The models that include stratospheric ozone depletion produce a larger cooling trend compared to models that do not. At these altitudes, the magnitude of the radiosonde trends is similar for the global and tropical averages, although the 2-sigma uncertainty in the tropical trend is about 20% larger than the global value. In the lower stratosphere and upper troposphere, the models show larger warming trends in the tropics compared with the global trends. At 150 hPa, the tropical trends with and without ozone depletion are between 0.1 and 0.2 K decade^{-1} more positive than the global trends. The crossover point between tropospheric warming and stratospheric cooling for the models including stratospheric ozone depletion is around 150 hPa for the global dataset and nearly 100 hPa for the tropical data. These changes are also reflected in the radiosonde observations, where the crossover point is estimated at 250 hPa globally and near 200 hPa in the tropics. Thompson and Solomon (2005)

found similar vertical profiles of temperature trends over 1979–2003 using both NCEP reanalysis and radiosonde datasets.

Below 200 hPa, the models and both satellite and radiosonde observations show statistically similar magnitudes in tropical warming trends, although the models are systematically warmer than the observations. The maximum warming trend in the tropical troposphere occurs near 300 hPa at around 0.3 K decade^{-1}, while the maximum warming trend in the global troposphere occurs near 200 hPa at around 0.2 K decade^{-1}. The larger warming in the tropics compared to the extratropics has been observed in previous model intercomparisons (e.g., IPCC, 2001) and the larger warming in the free troposphere compared to the surface was also identified in some observational trends and in the current group of IPCC models (Karl et al., 2006; Santer et al., 2005). The difference between the average models with and without ozone depletion in the upper troposphere and lower stratosphere (200 hPa–50 hPa) is less in the tropics compared to the global trends.

This analysis illustrates the importance of including ozone variations for accurate calculations of trends in the lower stratosphere and upper troposphere. The significant difference between the two groups of models suggests that inclusion of ozone trends is critical to correctly modeling the long-term temperature variability in the stratosphere and may also be important to tropospheric climate. It is also noted that during the 1979–1999 period, two large volcanic eruptions produced large temperature perturbations and thus increased the uncertainty of the trend calculation during this period. Thus, the inclusion of volcanic aerosol is also important for assessing long-term climate variations in the stratosphere.

5 21st century climate predictions

Long term changes in radiative forcing over the next few decades will continue to impact global mean temperature in both the troposphere and stratosphere. Because many of the chemical reactions that affect ozone are sensitive to stratospheric temperature, it

is important to establish an understanding of the range of possible future temperature trends to facilitate more realistic predictions of how ozone will change in the future.

The models used for the IPCC have been run with various emission scenarios for the 21st century. In this study, we will focus on the A2 and B1 scenarios from the Special Report on Emissions Scenarios (SRES, IPCC, 2000) that differ primarily in the emissions of well-mixed green house gases. In the A2 scenario, concentrations of CO_2 increase from today's value (~380 ppmv) to approximately 850 ppmv by 2100, while the B1 scenario reaches 550 ppmv by 2100 (IPCC, 2001). These two scenarios reflect the most likely extremes for CO_2 concentrations by the end of the century. The coupled models used for the 2001 IPCC report produce increases in global surface temperature of between 1.5 and 4.5 K by 2100 when forced with these scenarios.

Figure 10 shows a time series of temperature anomaly between 2000–2100 at 50 hPa from the fifteen models that submitted 21st century simulations. In these simulations, the future well-mixed GHG concentrations are specified by the A2 scenario, while ozone concentrations, which are not computed interactively, range from some type of ozone recovery to a constant value during the 21st century. While all model simulations show 50 hPa global temperatures declining over the 21st century, the range of predictions varies from −0.5 to −3.5 K by 2100. Differences in model ozone concentrations over the 21st century are likely responsible for some of the range in model predictions.

The relative uncertainty in model predictions of stratospheric temperature is further illustrated in Fig. 11, which shows the globally averaged temperature trend computed during the 21st century for the IPCC models using the A2 and B1 scenarios. The trends are calculated between 2010 and 2090 and thus reflect the range of possible temperature changes through the 21st century. In both the troposphere and stratosphere, the different emission scenarios produce significantly different trends. In the troposphere, the simulations using the A2 scenario show a surface warming near 0.3 K decade^{-1}, and increasing up to 0.5 K decade^{-1} at 300 hPa. The weaker forcing in the models using the B1 scenario produces a much smaller tropospheric response peaking at 0.25 K

ACPD
6, 7657–7695, 2006

EGU

decade^{-1} at 300 hPa. The crossover altitude between warming and cooling is independent of emission scenarios and occurs near 70 hPa. This is a similar crossover altitude as found in the 20th century simulations using the models that did not include ozone variations and mirrors the signature of well-mixed GHG forcing. In the stratosphere, the rate of cooling increases with increasing altitude up to around −0.7 K decade^{-1} for the A2 scenario and −0.4 K decade^{-1} for the B1 scenario. These simulations point to the changing nature of both the stratosphere and troposphere and the large role emissions play in shaping their future temperature.

It should be emphasized that these models do not include interactive chemistry and thus cannot accurately predict the interaction between decreasing chlorine levels that affect ozone concentrations and increasing greenhouse gases that affect temperature. While declines in stratospheric ozone also act to cool the stratosphere, at some point in the future global ozone levels will gradually begin to rise (WMO, 2003). In the stratosphere, higher ozone levels will increase the amount of stratospheric ozone heating which will at least partially offset the cooling due to increases in GHGs. Because ozone concentrations are sensitive to the background temperature field, understanding the complex interaction between changing constituent concentrations and temperature requires an evaluation of the coupling between chemistry, radiation and atmospheric dynamics (Cordero and Nathan, 2005; Tian and Chipperfield, 2005). One example of this interaction is how the large cooling rates present in the upper stratosphere decrease the temperature dependent ozone destruction and are forecast to produce a super recovery in ozone where future total column ozone levels are actually higher than pre-halogen levels (Eyring et al., 2006). It should be acknowledged that because these interactions are not resolved in the IPCC AOGCMs, accurate predictions of stratospheric temperature trends, especially those in the lower stratosphere, cannot be expected without reasonably accurate ozone predictions (Hare et al., 2004). In the present set of IPCC model simulations, the ozone forcing in the 21st century model experiments varies from constant ozone to a slow recovery by 2050.

Another challenge in accurately predicting stratospheric temperature in the 21st cen-

tury concerns future changes in stratospheric water vapor. At present, there is not a good understanding of how stratospheric water vapor will evolve in the future, nor the processes governing these changes. For this problem, coupled climate chemistry simulations that self consistently compute the interactions between radiatively active gases such as ozone and water vapor and large scale dynamics are again required (Austin et al., 2003).

How well do the IPCC models compare with models that include interactive chemistry? In model experiments with doubled CO_2 conditions including interactive ozone chemistry, substantial cooling is found throughout the middle atmosphere, with a maximum cooling of $\sim -3\,\mathrm{K\ decade^{-1}}$ near the stratopause and $\sim -1.5\,\mathrm{K\ decade^{-1}}$ at 10 hPa (Jonsson et al., 2004; Sigmond et al., 2004). In recent coupled chemistry climate model intercomparisons (Austin and Butchart, 2003; Eyring et al., 2006, 2005), the cooling trend at 10 hPa is about $-0.6\,\mathrm{K\ decade^{-1}}$ between 2000–2050. The weaker cooling trend is in line with increasing ozone concentrations through the first half of the 21st century, but is also of similar magnitude as the trends from the models used for the IPCC. In a recent coupled chemistry-climate model (CCM) intercomparison (Eyring et al., 2006), an A1b scenario is used for the 21st century simulations, which is a middle forcing between the A2 and B1 forcings. In comparison to Fig. 11, the average trend computed by the CCM models is $-0.6\,\mathrm{K\ decade^{-1}}$ at 10 hPa which falls within the A2 and B1 IPCC model trends.

Although there is some general agreement among models for how temperature will change in the future, there remains significant uncertainty regarding how well dynamical processes are resolved in climate models. It is recognized that stratospheric temperature changes result from both direct radiative forcing (e.g., CO_2, O_3, volcanic aerosol and water vapor) and dynamical circulation changes induced by tropospheric changes, and that forcing mechanisms are linearly additive (Ramaswamy et al., 2006). However, our understanding of how these interactions may change in the future is still poor (Nathan and Cordero, 2006[1]). In addition, various experiments using coupled cli-

[1]Nathan, T. R. and Cordero, E. C.: An ozone-modified refractive index for vertically propa-

mate chemistry models found that the inclusion of interactive chemistry can alter model meteorology (Austin and Butchart, 2003; Manzini et al., 2003; Tian and Chipperfield, 2005), coupling that was not included in the IPCC models. Finally, there remains significant uncertainty concerning dynamical processes associated with the parameterization of gravity waves and propagation of planetary waves in global models (e.g., Austin et al., 2003; Shaw and Shepherd, 2006[2]).

6 Discussion

Using MSU4 weighted temperature trends, Ramaswamy et al. (2006) recently attributed stratospheric temperature changes since 1979 to a combination of human and natural factors. Good agreement between models and observations were found when including well-mixed greenhouse gas changes, ozone changes and natural solar and volcanic changes. Each forcing contributed to the overall temperature-response time series. Their conclusions were based on results from a single model. Our findings generally support their conclusion across a wide range of models. However, our results also suggest that ozone and volcanic forcings need to be carefully evaluated and implemented in models. In particular, most models that included volcanic aerosols appear to have too much lower stratospheric (50 hPa) warming associated with Mt Pinatubo.

For many years there has been controversy over apparent differences in modeled and observed temperature trends in the free troposphere, comparing trends from radiosondes, satellites and models (e.g., NRC, 2004). The recent CCSP report (Karl et al., 2006) and the papers it cites (e.g., Fu et al., 2004) resolve many of these issues. Our findings also tend to support the conclusions of this report, that models and observed trends appear in agreement, within their respective uncertainties. However, the CCSP report also notes that in the tropics *"while almost all model simulations show*

gating planetary waves, J. Geophys. Res., submitted, 2006.

[2]Shaw, A. T. and Shepherd, T. G.: Angular momentum conservation and gravity wave drag parameterization: Implications for climate models, J. Atmos. Sci., submitted, 2006.

greater warming aloft, most observations show greater warming at the surface". Our results also support this conclusion. In particular they point to a real difference in the upper tropical troposphere. Since 1979 there seems to have been a real cooling trend in the radiosonde observations down to altitudes around 200 hPa, whereas in models it is almost impossible to get a cooling below 100 hPa. They all exhibit a typical moist-adiabatic type of response (see e.g., Karl et al., 2006). Although the cooling trend in radiosonde datasets could be up to 0.1 K decade^{-1} too large in this region (Randel and Wu, 2006) and radiosonde trends have many uncertainties, this difference appears real.

Reasons for this difference could be associated with convection schemes in the models and/or their upper tropospheric water vapor feedback and/or resolution in the upper troposphere. Much of the upper tropical troposphere (often termed the Tropical Tropopause Transition layer or sub-stratosphere) is above typical altitudes of convective outflow (e.g., Folkins et al., 1999; Gettelman and Forster, 2002; Thuburn and Craig, 2000) and as such may behave more like part of the stratosphere (Forster et al., 1997; Thuburn and Craig, 2000). Forster and Collins (2004) also suggest that although the water vapor feedback is generally well understood, the water vapor feedback in the upper troposphere may not be particularly well represented by model simulations of the Mt Pinatubo eruption. In the AOGCMs, relative humidity stays more or less constant with altitude (Karl et al., 2006). If this is not occurring in reality or if stratospheric radiative processes are playing more of a dominant role in the 200–100 hPa region than the AOGCMs suggest, then temperature trends could be more negative than typical models suggest in this region. Randel et al. (2006) suggest that recent temperature changes around the tropical tropopause could have been caused by a radiative response to a combination of ozone and water vapor changes; perhaps similar mechanisms are controlling the observed temperature trends in the 200 hPa–100 hPa region and current AOGCMs are unable to capture these mechanisms. As the water vapor feedback from this region is very important for tropospheric climate evolution, our work suggests the need for a more focused effort to try and understand the large scale pro-

ACPD
6, 7657–7695, 2006

cesses governing temperature trends in the region, as well as efforts to make sure that AOGCMs can adequately simulate these responses.

7 Conclusions

AOGCM simulations submitted for the Fourth Assessment Report of the IPCC are analyzed to assess the ability of these models to simulate stratospheric variability and trends. Model temperature simulations between 1979–1999 are compared with NCEP reanalysis, and show that model to model variability is larger in the stratosphere compared to the troposphere, even when natural variability is considered. Model simulations that include volcanic aerosols are necessary to reproduce the observed interannual variability in the stratosphere, although most models that include volcanic aerosols tend to over predict the temperature response at 50 hPa. Although a cold temperature bias in relation to NCEP is seen in a majority of the models throughout the stratosphere, the presence of a cold pole bias is only evident at 10 hPa during the winter. At 50 hPa, most models are within the NCEP variability in the NH winter, and within or warmer than the NCEP variability in the SH winter. However, at 10 hPa, about half the models are between 10–15 K colder than NCEP. It appears that this difference is related to representation of the stratosphere within each model. In models with few stratospheric levels and a relatively low model top, the cold pole bias is about 9 K larger than the models with more stratospheric levels and a higher model top. This comparison suggests that in the present collection of models used by the IPCC, about half the models do not possess a high enough model top to accurately simulate stratospheric variability at 10 hPa. This shortcoming is expected to potentially affect other fields at 10 hPa and is likely to contribute to unrealistic variability at lower levels.

Stratospheric temperature trends in models are compared to existing radiosonde and satellite observed trends. In general, the models tend to underestimate the cooling trends in the stratosphere observed over the last forty years. The cooling of the stratosphere, which is largely controlled by declines in stratospheric ozone and in-

ACPD
6, 7657–7695, 2006

creases in tropospheric GHGs, is only well simulated in models that include ozone depletion over the last thirty years. However, in models that neglect ozone depletion, the temperature trends in the stratosphere do not show enough cooling. The largest discrepancy between model trends and observations is found in the upper troposphere and lower stratosphere, where even models that include ozone depletion do not cool as much as the observations. This discrepancy appears largest between 1979–1999, in tropical latitudes (30° N–30° S) between 100–200 hPa. Although tropical radiosonde observations may themselves posses a spurious cooling trend, our analysis suggests that these differences appear real and should motivate further investigations to identify the source of these differences.

In the 21st century, model simulations using an A2 emission scenario all show the stratosphere continuing to cool, but with a wide range of projections. It is suggested, although not verified here, that differences in future ozone projections are responsible for a significant proportion of this range. Model simulations also show that the strength of cooling in the stratosphere and warming in the troposphere are dependent on the emission scenario, but that the altitude of the crossover point between warming and cooling does not appear to change with emission scenario. These results illustrate how sensitive stratospheric temperature trends are to future well-mixed GHG concentrations

Acknowledgements. We gratefully acknowledge the international modeling groups for providing their data for analysis, the Program for Climate Model Diagnosis and Intercomparison (PCMDI) for collecting and archiving the model data, the JSC/CLIVAR Working Group on Coupled Modeling (WGCM) and their Coupled Model Intercomparison Project (CMIP) and Climate Simulation Panel for organizing the model data analysis activity, and the IPCC WG1 TSU for technical support. The IPCC Data Archive at Lawrence Livermore National Laboratory is supported by the Office of Science, U.S. Department of Energy. E. C. Cordero is supported by NSF's Faculty Early Career Development Program (CAREER), Grant ATM-0449996 and NASA's Living with a Star, Targeted Research and Technology Program, Grant LWS04-0025-0108. P. M. Forster is supported by a Roberts Research Fellowship.

References

Austin, J. and Butchart, N.: Coupled chemistry-climate model simulations for the period 1980 to 2020: ozone depletion and the start of ozone recovery, Quart. J. R. Met. Soc., 129, 3225–3249; doi:10.1256/qj.02.203, 2003.

Austin, J., Shindell, D., Beagley, S. R., et al.: Uncertainties and assessments of chemistry-climate models of the stratosphere, Atmos. Chem. Phys., 3, 1–27, 2003.

Cordero, E. C. and Nathan, T. R.: A New Pathway for Communicating the 11-Year Solar Cycle Signal to the QBO, Geophys. Res. Lett., 32, L18805, doi:10.1029/2005GL023696, 2005.

Eyring, V., Butchart, N., Waugh, D. W., et al.: Assessment of coupled chemistry-climate models:1. Evaluation of dynamics, transport characteristics and ozone, J. Geophys. Res., in press, 2006.

Eyring, V., Harris, N. R. P., Rex, M., et al.: A strategy for process-oriented validation of coupled chemistry-climate models, Bull. Am. Met. Soc., 86, 1117–1133, 2005.

Folkins, I., Lowewenstein, M., Podolske, J. R., Oltmans, S. J., and Proffitt, M. H.: A barrier to vertical mixing at 14 km in the tropics: Evidence from ozonesondes and aircraft measurements, J. Geophys Res., 104, 22 095–22 102, 1999.

Forster, P. M. d. F., Blackburn, M., Glover, R., and Shine, K. P.: An examination of climate sensitivity for idealised climate experiments in an intermediate general circulation model, Clim. Dyn., 16, 833–849, 2000.

Forster, P. M. d. F. and Collins, M.: Quantifying the water vapour feedback associated with post-Pinatubo global cooling, Clim. Dyn., 23, 207–214, 2004.

Forster, P. M. d. F., Freckleton, R. S., and Shine, K. P.: On aspects of the concept of radiative forcing, Clim. Dyn., 13, 547–560, 1997.

Forster, P. M. d. F. and Shine, K. P.: Assessing the climate impact and its uncertainty for trends in stratospheric water vapor, Geophys. Res. Lett., 29, doi:10.1029/2001GL013909, 2002.

Free, M. and Angell, J. K.: Effect of volcanoes on the vertical temperature profile in radiosonde data, J. Geophys. Res., 107(D10), 4101, doi:1029/2001JD001128, 2002.

Free, M., Angell, J. K., Durre, I., et al.: Using first differences to reduce inhomogeneity in radiosonde temperature datasets, J. Clim., 17, 4171–4179, 2004.

Free, M., Seidel, D. J., Angel, J. K., et al.: Radiosonde atmospheric temperature products for assessing climate (RATPAC): a new dataset of large-area anomaly time series, J. Geophys. Res., 110, doi:10.1029/2005JD006169, 2005.

Fu, Q., Johanson, C. M., Warren, S. G., and Seidel, D. J.: Contribution of stratospheric cooling to satellite-inferred tropospheric temperature trends, Nature, 429, 55–58, 2004.
Gettelman, A. and Forster, P. M. d. F.: Definition and climatology of the tropical tropopause layer, J. Meteor. Soc. Japan, 80, 911–924, 2002.
Gillett, N. P., Allen, M. R., McDonald, R. E., et al.: How linear is the Arctic Oscillation response to greenhouse gases?, J. Geophys. Res., 107, doi:10.1029/2001JD000589, 2002.
Gillett, N. P. and Thompson, D. W.: Simulation of recent southern hemisphere climate change, Science, 302, 273–275, 2003.
Haigh, J. D.: Climate variability and the influence of the sun, Science, 294, 2109–2111, 2001.
Haigh, J. D., Blackburn, M., and Day, R.: The response of tropospheric circulation to perturbations in lower stratospheric temperature, J. Clim., 18, 3672–3691, 2005.
Hamilton, K., Wilson, R. J., and Hemler, R. S.: Middle Atmosphere Simulated with High Vertical and Horizontal Resolution Versions of a GCM: Improvements in the Cold Pole Bias and Generation of a QBO-like Oscillation in the Tropics, J. Atmos. Sci., 56, 3829–3846, 1999.
Hare, S. H. E., Gray, L. J., Lahoz, W. A., O'Neill, A., and Steenman-Clark, L.: Can stratospheric temperature trends be attributed to ozone depletion?, J. Geophys. Res., 109, doi:1029/2003JD003897, 2004.
Houghton, J. T., Ding, Y., Griggs, D. J., et al. (Eds.): Climate Change 2001: The Scientific Basis, Contribution of Working Group I to the Third Assessment Report of the Intergovernmental Panel on Climate Change, Cambridge University Press, Cambridge, UK, 881 pp, 2001.
IPCC: Emissions Scenarios, Special Report of the Intergovernmental Panel on Climate Change, Cambridge University Press, Cambridge, UK, 2000.
IPCC: Climate Change 2001: The Scientific Basis. Contribution of Working Group I to the Third Assessment Report of the Intergovernmental Panel on Climate Change, Cambridge University Press, Cambridge, UK, 2001.
Jonsson, A. I., Grandpre, J. d., Fomichev, V. I., McConnell, J. C., and Beagley, S. R.: Doubled CO2-induced cooling in the middle atmosphere: Photochemical analysis of the ozone radiative feedback, J. Geophys. Res., 109, doi:10.1029/2004JD005093, 2004.
Karl, T. R., Hassol, S. J., Miller, C. D., and Murray, W. L. (Ed.): Temperature Trends in the Lower Atmosphere: Steps for Understanding and Reconciling Differences, The climate change science program and the subcommittee on global change research, Washington, D.C., USA, 2006.
Kistler, R. et al.: The NCEP-NCAR 50-year reanalysis: Monthly means CD-ROM and docu-

mentation, Bull. Am. Met. Soc., 82, 247–267, 2001.
Manzini, E., Steil, B., Bruhl, C., Giorgetta, M. A., and Kruger, K.: A new interactive chemistry climate model. 2: Sensitivity of the middle atmosphere to ozone depletion and increase in greenhouse gases: Implications for recent stratospheric cooling, J. Geophys. Res., 108, 4429, doi:10.1029/2002JD002977, 2003.
Mears, C. A., Schabel, M. C., and Wentz, F. J.: A reanalysis of the MSU channel 2 tropospheric temperature record, J. Clim., 16, 3650–3664, 2003.
Miller, R. L., Schmidt, G. A., and Shindell, D. T.: Forced variations of annular modes in the 20th century IPCC AR4 simulations, J. Geophys. Res., in press, 2006.
Newman, P. A. and Nash, E. R.: The unusual southern hemisphere stratosphere winter of 2002, J. Atmos. Sci., 62, 614–628, 2005.
NRC: Climate data records from environmental satellites, National Academy Press, 2004.
Pawson, S., Kodera, K., Hamilton, K., et al.: The GCM-Reality intercomparison project for SPARC (GRIPS): Scientific issues and initial results, Bull. Amer. Meteor. Soc., 81, 781–796, 2000.
Ramaswamy, V., Chanin, M.-L., Angell, J., et al.: Stratospheric temperature trends: observations and models simulations, Rev. Geophys., 39, 71–122, 1999RG000065, 2001.
Ramaswamy, V., Schwarzkopf, M. D., Randel, W., et al.: Anthropogenic and natural influences in the evolution of lower stratospheric cooling, Science, 311, 1138–1141, 2006.
Randel, W., Udelhofen, P., Fleming, E. L., et al.: The SPARC Intercomparison of middle-atmosphere climatologies, J. Clim., 17, 986–1003, 2004.
Randel, W. J. and Wu, F.: Biases in stratospheric and troposheric temperature trends derived from historical radiosonde data, J. Clim., in press, 2006.
Randel, W. J., Wu, F., Nedoluha, H. G., and Forster, P. M. d. F.: Decreases in stratospheric water vapor since 2001: Links to changes in the tropical tropopause and the Brewer-Dobson circulation, J. Geophys. Res., in press, 2006.
Rind, D.: Climatology: The sun's role in climate variations, Science, 296, 673–677, 2002.
Rind, D., Shindell, D., Perlwhitz, J., and Lerner, J.: The Relative Importance of Solar and Anthropogenic Forcing of Climate Change between the Maunder Minimum and the Present, J. Clim., 17, 906–929, 2004.
Santer, B. D., Sausen, R., Wigley, T. M. L., et al.: Behavior of tropopause height and atmospheric temperature in models, reanalyses and observations: Decadal changes, J. Geophys. Res., 108, doi:10.1029/2002JD002258, 2003a.

Santer, B. D., Wehner, M. F., Wigley, T. M. L., et al.: Contributions of anthropogenic and natural forcing to recent tropopause height changes, Science, 301, 479–483, 2003b.
Santer, B. D., Wigley, T. M. L., Mears, C., et al.: Amplification of surface temperature trends and variability in the tropical atmosphere, Science, 309, 1551–1556, doi:10.1126/science.1114867, 2005.
Seidel, D. J., Angell, J. K., Christy, J., et al.: Uncertainty in signals of large-scale climate variations in radiosonde and satellite upper-air temperature datasets, J. Clim., 2225–2240, 2004.
Shindell, D. T. and Schmidt, G. A.: Southern hemisphere climate response to ozone changes and greenhouse gas increases, Geophys. Res. Lett., 31, doi:10.1029/2004GL020724, 2004.
Shine, K. P., Bourqui, M. S., Forster, P. M. F., et al.: A comparison of model-simulated trends in stratospheric temperature, Q. J. R. Met. Soc., 129, 1565–1588; doi:10.1256/qj.02.186, 2003.
Sigmond, M., Siegmund, P. C., Manzini, E., and Kelder, H.: A simulation of the separate climate effects of middle-atmosphere and tropospheric CO_2 doubling, J. Clim., 17, 2352–2367, 2004.
Stenchikov, G., Robock, A., Ramaswamy, V., et al.: Arctic oscillation response to the 1991 Mount Pinatubo eruption: effects of volcanic aerosols and ozone depletion, J. Geophys Res., 107, doi:10.1029/2002JD002090, 2002.
Stuber, N., Ponater, M., and Sausen, R.: Is the climate sensitivity to ozone perturbations enhanced by stratospheric water vapor feedback, Geophys. Res. Lett., 28, 2887–2890, 2001.
Tett, S. F. B., Mitchell, J. F. B., Parker, D. H., and Allen, M. R.: Human influence on the atmospheric vertical temperature structure: Detection and observations, Science, 274, 1170–1173, 1996.
Thompson, D. W., Baldwin, M. P., and Solomon, S.: Stratosphere-troposphere coupling in the Southern Hemisphere, J. Atmos. Sci., 62, 708–715, 2005.
Thompson, D. W. and Solomon, S.: Recent stratospheric climate trends as evidenced in radiosonde data:Global structure and tropospheric linkages, J. Clim., 18, 4785–4795, 2005.
Thorne, P. W., Parker, D. E., Tett, S. F. B., et al.: Revisiting radiosonde upper air temperature from 1958 to 2002, J. Geophys. Res., 110, doi:10.1029/2004JD005753, 2005.
Thuburn, J. and Craig, G. C.: Stratospheric influence on tropopause height: The radiative constraint, J. Atmos. Sci., 57, 17–28, 2000.

Tian, W. and Chipperfield, M. P.: A new coupled chemistry-climate model for the stratosphere: The importance of coupling for future O3-climate predictions, Q. J. R. Met. Soc., 131, 281–303, 2005.
WMO: Scientific assessment of ozone depletion: 2002, Global ozone research and monitoring project, Report number 47, 498, 2003.

Table 1. Specific forcings and details of the vertical model structure for each model submitted to the IPCC. The forcing terms are for the 20th century simulation (20CM3) where GHG represent increases in well-mixed greenhouse gases, volcanic refers to volcanic aerosols, ozone refers to changes in stratospheric ozone and solar refers to changes in solar irradiance. The term Z-top refers to the approximate altitude of the top of the model, S-lev refers to the number of stratospheric levels. Models with a top at or above 45 km are classified as "High" while models with tops below that level are classified as "Low".

Model	GHG	Volcanic	Ozone	Solar	Z-top	S-lev	Model top
BCCR-BCM2.0	Y	N	N	N	33	5	Low
CCSM3	Y	Y	Y	Y	40	7	Low
CGCM3.1(T47)	Y	N	N[b]	?	49	11	High
CNRM-CM3	Y	N	N[b]	N	76	17	High
CSIRO-Mk3.0	Y	N[a]	Y	N	38	3	Low
ECHAM5/MPI-OM	Y	N	Y	?	29	4	Low
FGOALS-g1.0	Y	N	N[b]	Y	45	9	High
GFDL-CM2.0	Y	Y	Y	Y	35	3	Low
GFDL-CM2.1	Y	Y	Y	Y	35	3	Low
GISS-AOM	Y	N	N	N	33	3	Low
GISS-EH	Y	Y	Y	Y	67	9	High
GISS-ER	Y	Y	Y	Y	67	9	High
INM-CM3.0	Y	N[a]	N	N	32	6	Low
IPSL-CM4	Y	N	N	N	32	7	Low
MIROC3.2(hires)	Y	Y	Y	Y	45	19	High
MIROC3.2(medres)	Y	Y	Y	Y	67	6	High
MRI-CGCM2.3.2	Y	N[a]	N	Y	54	8	High
PCM	Y	Y	Y	Y	43	7	Low
UKMO-HadCM3	Y	N	Y	?	39	5	Low

N[a] = Documentation claims inclusion of volcanic aerosols, but Fig. 7 shows no temperature response to volcanic eruptions.

N[b] = Documentation claims inclusion of ozone trends, but Fig. 8 shows little cooling in the lower stratosphere.

ACPD
6, 7657–7695, 2006

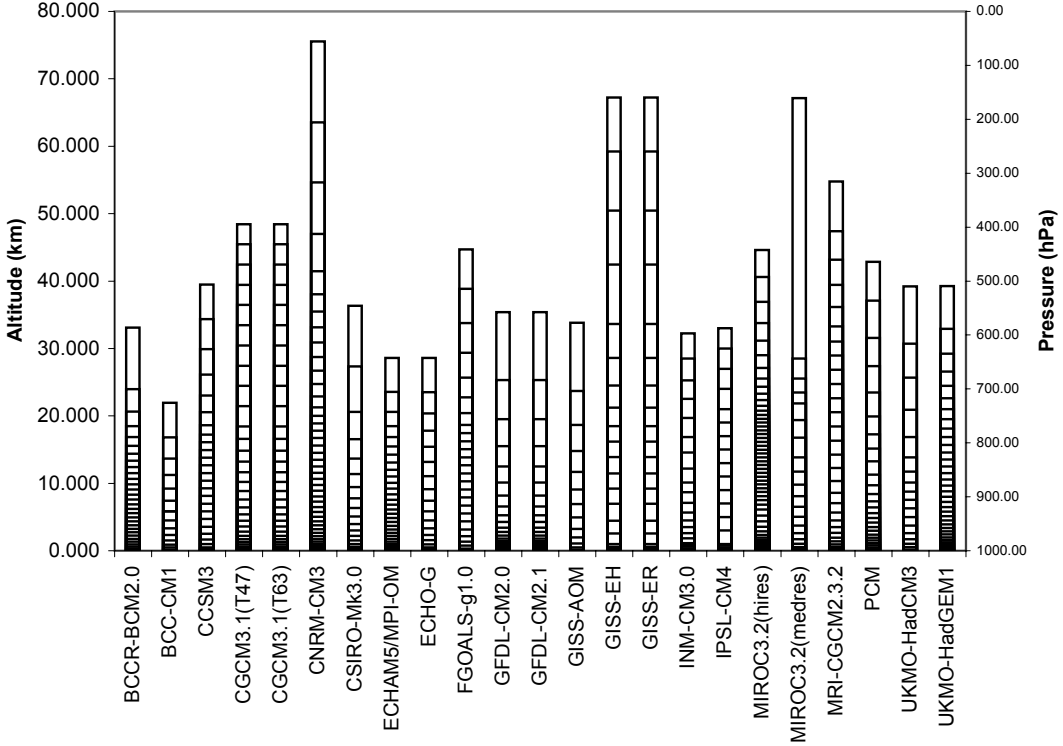

Fig. 1. Approximate altitude of the vertical levels for models submitted to the IPCC AR4.

ACPD
6, 7657–7695, 2006

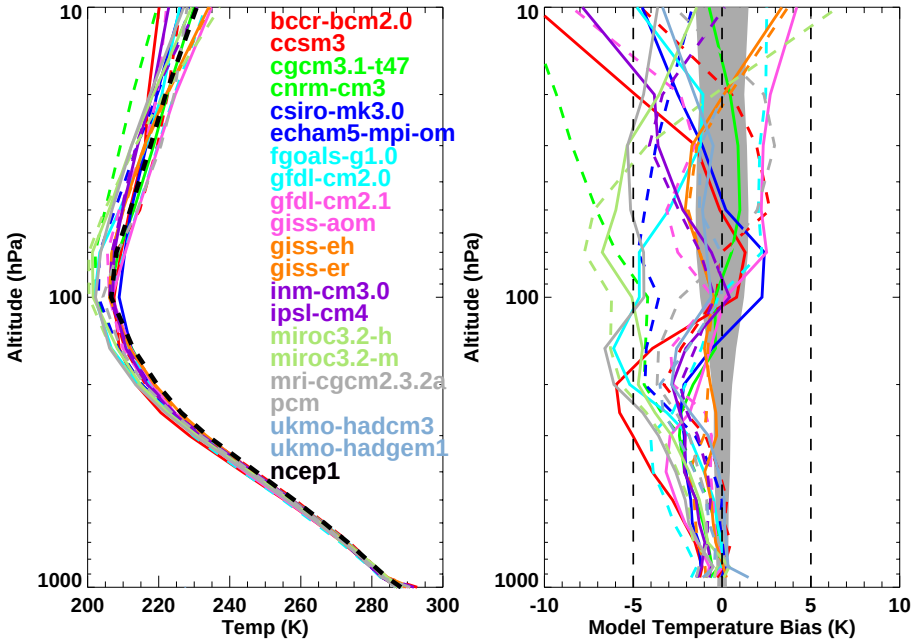

Fig. 2. Globally averaged temperature (left) and model temperature bias (right) between 1979–1999 for the climate models and the NCEP reanalysis. The lines identifying each model alternate between solid and dashed, so that for each color the first listed model uses a solid line and the second listed model a dashed line. The gray shading in the model temperature bias plot shows NCEP plus and minus 2 standard deviations around the climatological mean.

ACPD
6, 7657–7695, 2006

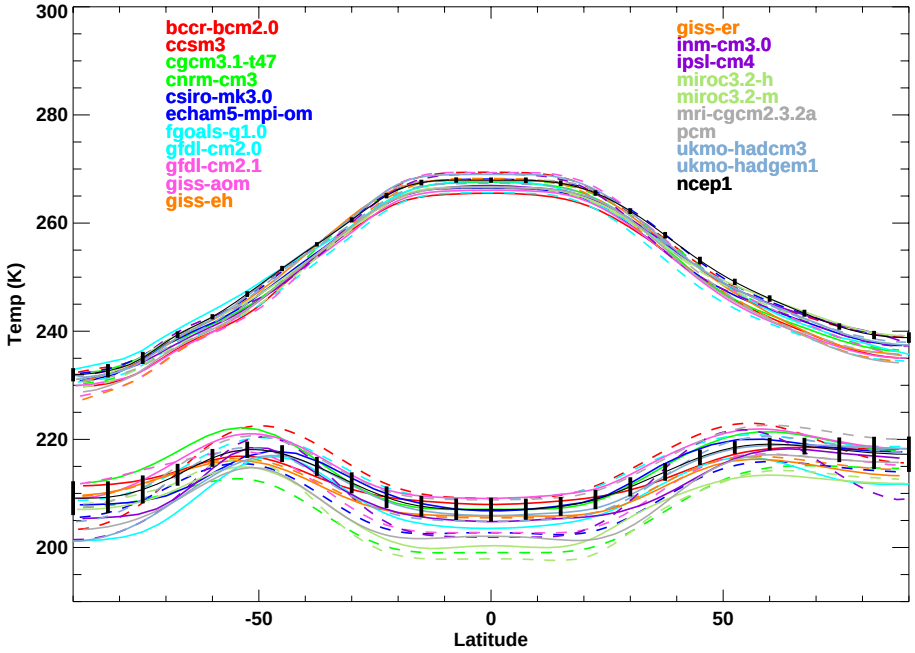

Fig. 3. Zonally and annually averaged temperature at 500 hPa (upper) and 50 hPa (lower) between 1979–1999 from the climate models and NCEP. The 2-σ variation in the NCEP reanalysis is shown in the heavy black vertical lines, and the colors are as in Fig. 2.

ACPD
6, 7657–7695, 2006

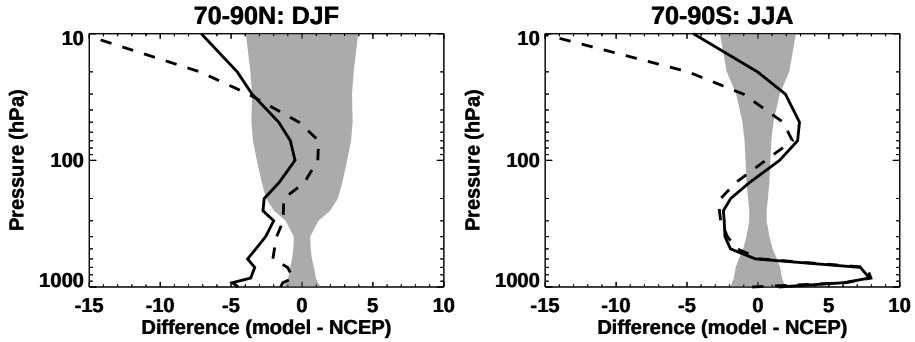

Fig. 4. Zonally averaged temperature difference in K between the models and NCEP in the high latitude winter hemisphere averaged between 1979–1999. Models with a high top are averaged together and displayed with a solid line and models with a low top are averaged together and displayed with a dashed line. The differences are computed for DJF (left) and JJA (right). The gray shading indicates the 1 sigma standard deviation in the NCEP reanalysis.

ACPD
6, 7657–7695, 2006

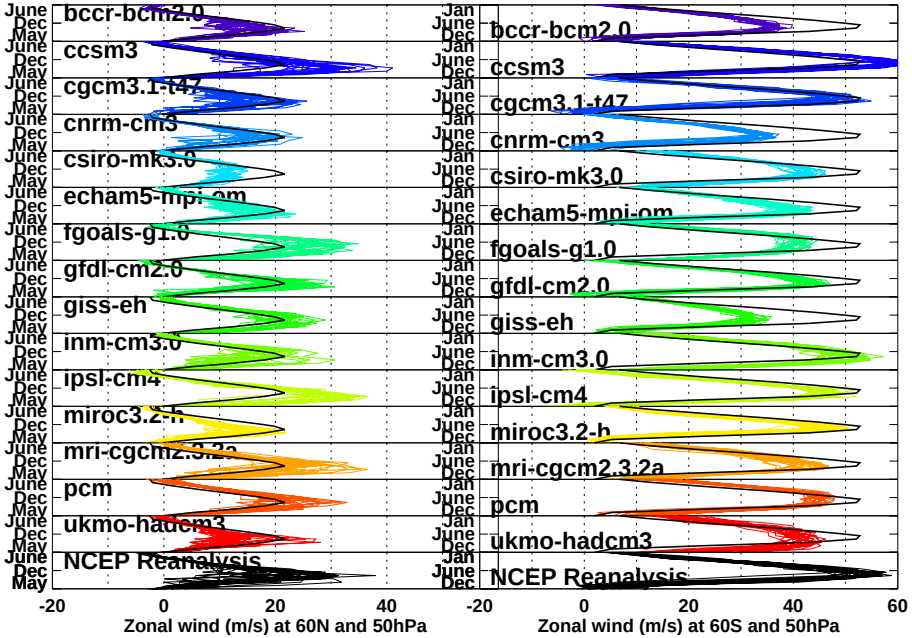

Fig. 5. Time series of zonally averaged zonal wind at 60◦ N (left) and 60° S (right) at 50 hPa between the year 1979–1999 for a subset of the submitted IPCC models and the NCEP reanalysis. Each of the 20 years of data is plotted on top of each other and compared to the 20 year mean NCEP reanalysis given in the black bold line.

ACPD
6, 7657–7695, 2006

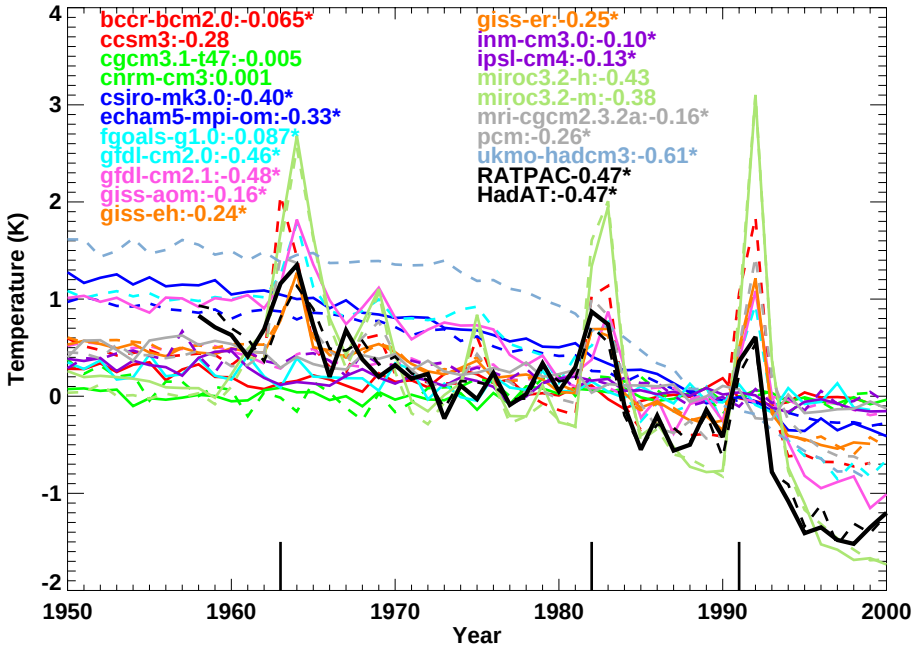

Fig. 6. Time series of globally averaged annual temperature anomaly averaged at 50 hPa. The solid vertical black lines indicate major volcanic eruptions and the bold lines (solid and dashed) represent the radiosonde observations from RATPAC-A and HadAT respectively. Next to each model is the linear temperature trend in K decade^{-1} calculated between 1958–1999, and the lines alternate from solid to dashed as in Fig. 2. Models with statistically significant trends are indicated with asterisk (*) after the trend.

ACPD
6, 7657–7695, 2006

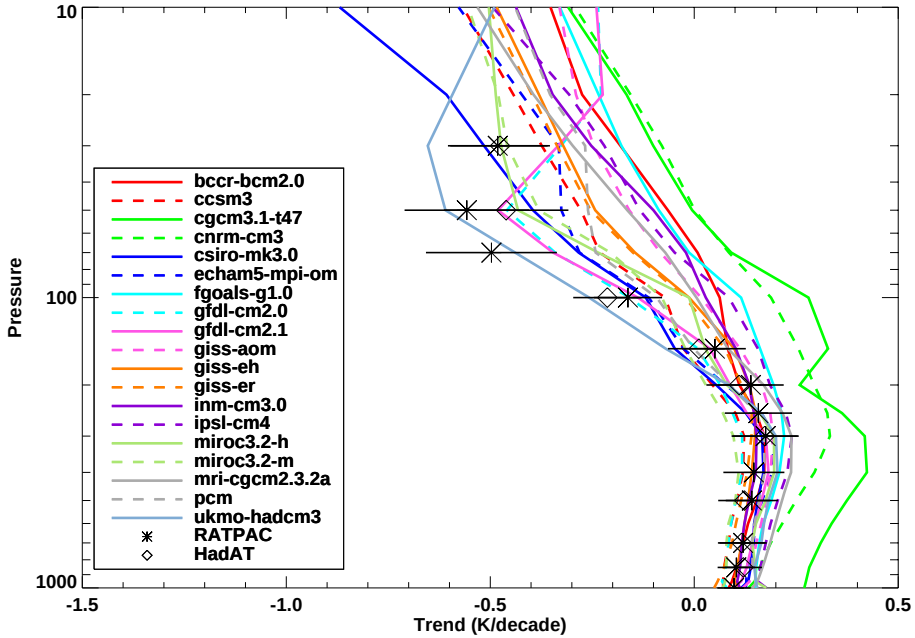

Fig. 7. The vertical distributions of model average global temperature trends in K decade^{-1} are calculated between 1958–1999. The radiosonde observations are given by the star and diamond symbols, and the thin horizontal line corresponds to their 2-sigma variation.

ACPD
6, 7657–7695, 2006

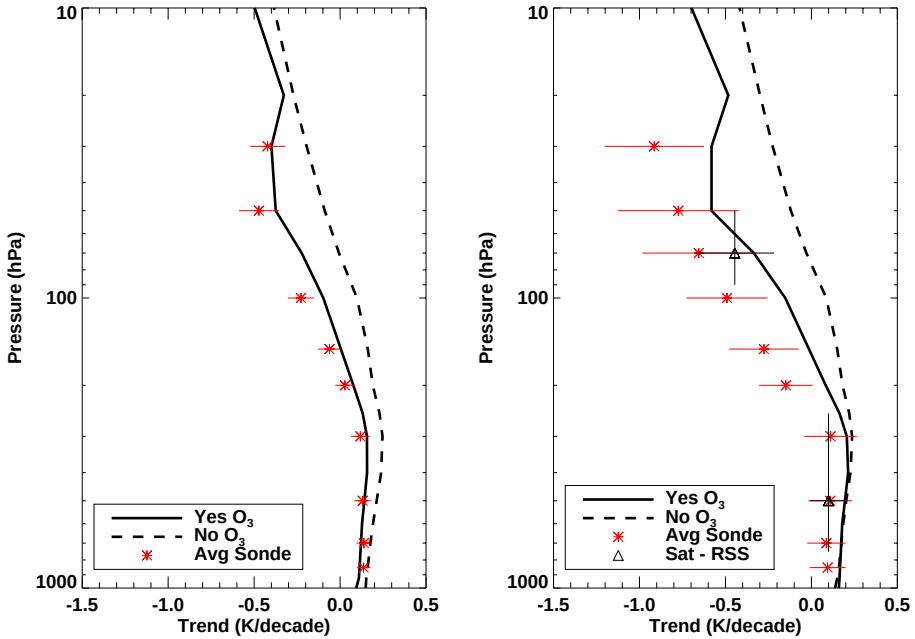

Fig. 8. The model average global temperature trend calculated between 1958–1999 (left) and 1979–1999 (right). The solid (dashed) lines represent trends averaged from models with (without) stratospheric ozone depletion. Average radiosonde trends and their 2-sigma variation are given by the red stars and the thin horizontal lines respectively. In the 1979–1999 trend, the satellite observations are given by the triangle symbol, where the thin horizontal line represents the 2-sigma variation in temperature and the thin vertical line represents the approximate vertical range of the observations.

ACPD
6, 7657–7695, 2006

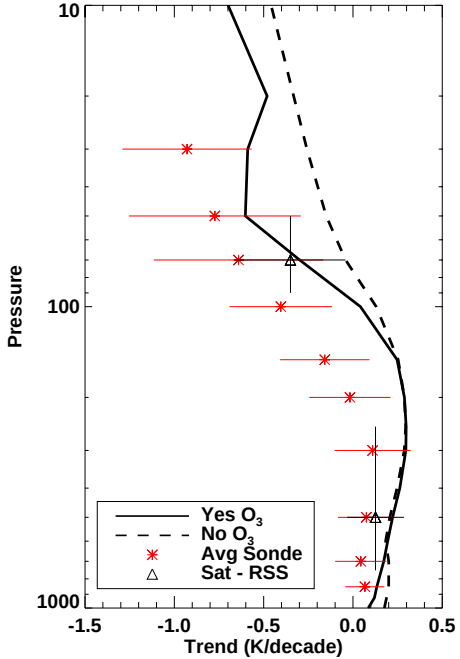

Fig. 9. As in Fig. 8 except for the tropical trend (30° N–30° S) between 1979–1999 trend. Satellite observations are given by the triangle symbol, where the thin vertical line represents the 2-sigma uncertainty and the thin vertical line represents the approximate vertical range of the observations.

ACPD
6, 7657–7695, 2006

EGU

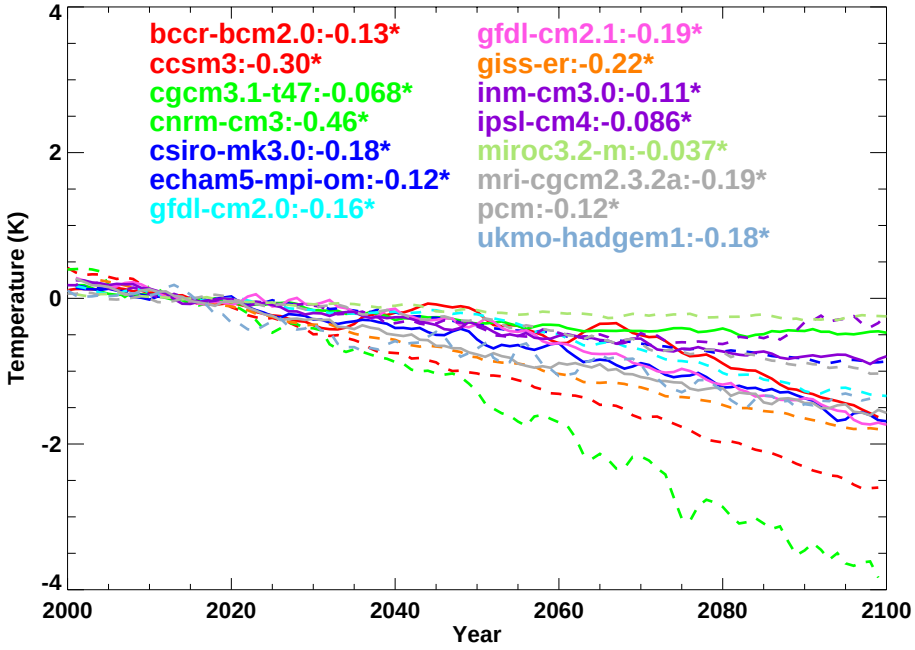

Fig. 10. Time series of global averaged temperature anomaly at 50 hPa between 2000–2100 from the A2 IPCC model simulations, where the lines alternate from solid to dashed as in Fig. 2. The temperature anomaly is computed with respect to temperatures between 2010 and 2020, and the temperature trend computed between 2010 and 2090 is given in K decade^{-1} next to the name of each participating model. Models with statistically significant trends are indicated with an asterisk (*) after the trend.

ACPD
6, 7657–7695, 2006

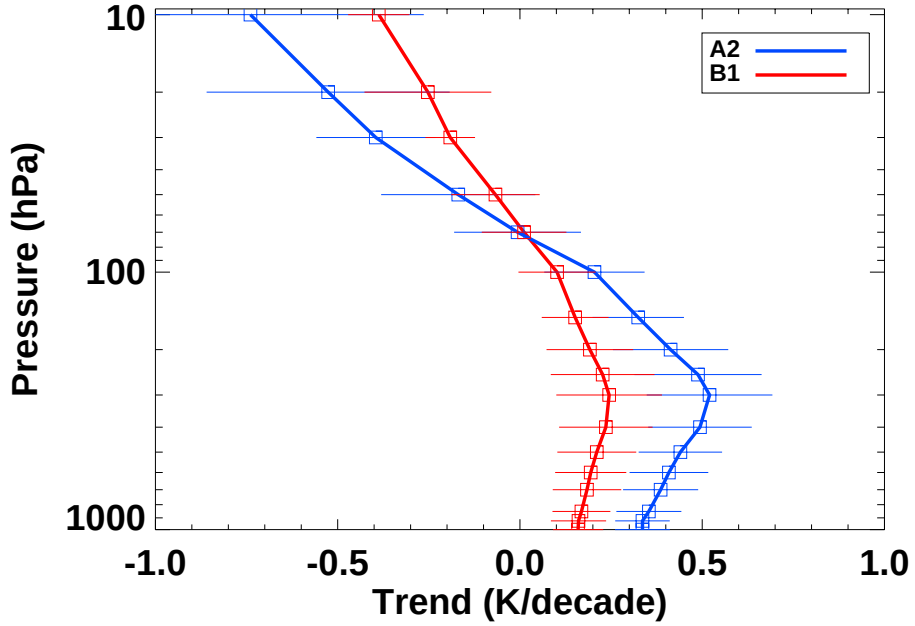

Fig. 11. Global and annual-mean temperature trends computed between 2010–2090 from the IPCC models using the A2 and B1 emission scenarios. The boxes indicate the average trend computed for all models while the thin horizontal lines indicate the range of model calculated trends.

ACPD
6, 7657–7695, 2006